Dynamics and statics of sodium-halide crystals

V. V. S. Nirwal and R. K. Singh
Department of Postgraduate Studies and Research in Physics, University of Jabalpur, Jabalpur 482001, India
(Received 9 August 1978; revised manuscript received 30 March 1979)

A consistent and comprehensive calculation has been performed to describe the dynamics and statics of sodium-halide crystals using a well-known three-body-force shell model (TSM). The computed results on the phonon dispersion, two-phonon Raman and infrared spectra, Debye-temperature variations, dielectric and photoelastic behaviors, harmonic and anharmonic elastic constants, cohesive energy, relative stability, and phase-transition, have shown a reasonably good agreement with their accurately measured data. All these predictions have made use of the same set of TSM parameters throughout. The possible sources of improvements have also been indicated. In view of its overall success, TSM has been regarded as an adequate and appropriate model for the description of lattice-mechanical properties of ionic crystals.

I. INTRODUCTION

The lattice dynamics of ionic crystals has been most extensively studied with several phonon models[1–7] and microscopic theories.[8–14] A survey of these literatures reveals that the phonon models have developed from the rigid-ion model[1] through rigid-shell model[2] (RSM) to three-body-force shell model[7] (TSM) in an attempt to describe the dielectric and dynamical behaviors of lattices obtained experimentally by inelastic neutron scattering. The efforts devoted to explain the elastic and static properties have also led to the development of some models.[15–17] However, none of these models is adequate to account simultaneously for all the properties cited above. It is only recently that the RSM framework has been extended to include the effect of short- and long-range three-body forces owing their origin to the deformation of electron shells. This has resulted in several useful variants of the RSM, namely, the breathing,[4] deformable,[5] and three-body-force[7] shell models. The first two of them are almost identical[18] and introduce short-range three-body-force effects in the RSM. The third model (TSM) has been developed by incorporating the effect of long-range three-body forces in the RSM framework. All these models have been applied to several ionic crystals with considerable success in dynamical descriptions.

Recently, Basu and co-workers,[19,20] have tried to explain both the lattice statics and dynamics of some ionic crystals by the deformable shell model[5] (DSM). The motivation for such work was derived from the remark of Cochram that a truly satisfactory model must explain the dynamics as well as the statics of a crystal. The descriptions obtained by them are although more or less satisfactory but their model is subject to some limitations. The three-body forces employed in the DSM are short range in nature and their representation is based on the approximate formulation of Sarkar and Sengupta.[21] Also, these forces are inadequate to account for the Cauchy violations and the optical vibrations along the [111] direction as recently pointed out by Laplaze.[22] Further, these forces have no effect on the zone-center vibration frequencies and hence the DSM framework does not go beyond the RSM in respect to accounting for the dielectric properties. In contrast, the three-body forces employed in the TSM are of long-range character and their formulation is based on the quantum-mechanical analysis of Löwdin[15] and Lundqvist.[16] Moreover, these forces take proper account of the Cauchy violations[15,16] and dielectric properties[23,24] and have considerable influence on the optical vibrations along the [111] direction.

The effect of long-range three-body forces on both the dynamics and statics of ionic crystals has not been analyzed so far. The chief concern of the present paper is thus to perform a comprehensive and consistent calculation of the lattice static and dynamic properties of sodium halides which are the simplest ionic crystals. These calculations will include cohesive energy, relative stability, phase-transition pressure and volume, phonon-dispersion relations, Debye-temperature variations, two-phonon Raman and infrared (ir) spectra, third-order elastic (TOE) constants, pressure derivatives of effective second-order elastic (SOE) constants, and dielectric and photoelastic behaviors. The choice of the solids under consideration is motivated by the fact that a wealth of accurately measured data on these properties is available only for the sodium-halide family. It is interesting to note that the agreement between theoretical and experimental results is generally good in almost all the cases.

A brief description of TSM theory approached in the present calculations is given in Sec. II. The results of its application to dynamic and static properties are collected in Sec. III. A summary of the

results together with the conclusions drawn from them is presented in Sec. IV.

II. TSM FORMALISM

The present TSM formalism has been derived by regarding the crystal energy as consisting of long-range Coulomb and three-body interactions (TBI) and short-range overlap repulsion of Born-Mayer type. Its relevant expression per unit cell is written

$$\Phi(r)=\frac{Z^2e^2}{r}\alpha_M+\frac{nZ^2e^2}{r}\alpha_M f(r)+nbe^{-r/\rho} \ , \tag{1}$$

where Ze is the ionic charge, α_M ($=-1.7476$) is the Madelung constant, n represents the number of nearest neighbors, $f(r)$ is a function that depends on the overlap integrals (Löwdin[16]) and measures the size difference of ions, and b and ρ are the usual strength and hardness parameters. The incorporation of this interaction potential in the RSM framework (Woods *et al.*[2]) leads to the following secular equation:

$$|D(q)-mIw^2|=0 \ , \tag{2}$$

for the vibration frequencies (w). The corresponding dynamical matrix is given by (Singh and Chandra[25])

$$D(q)=(\underline{R}+\underline{Z}'\underline{C}'\underline{Z}')-(\underline{R}+\underline{Z}'\underline{C}'\underline{Y}') \times(\underline{R}+\underline{K}+\underline{Y}'\underline{C}'\underline{Y}')^{-1}(\underline{R}^T+\underline{Y}'\underline{C}'\underline{Z}') \ , \tag{3}$$

where $\underline{R}$ is the short-range interaction matrix due to the overlap repulsion between the shells of nearest neighbors (nn) as well as of the next-nearest-neighbors (nnn). $\underline{K}$ is a diagonal matrix representing the force constant between the core and shell of the ions. The original core and shell charges (X,Y) of the RSM have been modified to (X',Y') given by

$$Z'=Z\left[1+\frac{2nf_0}{Z}\right]^{1/2}=X'+Y'=xZ'+yZ' \ , \tag{4}$$

and x and y as the reduced core and shell charge parameters such that $x+y=\pm1$.

Also, the modified long-range Coulomb interaction matrix is given by

$$\underline{C}'=\underline{C}+(Zr_0f_0'/Z'^2)\underline{V} \ , \tag{5}$$

with $\underline{C}$ and $\underline{V}$ as the Coulomb and three-body interaction matrices determined by Kallermann[1] and Verma and Singh,[7] respectively. Subjecting the dynamical matrix given by Eq. (3) to the long-wavelength limit, we have obtained the following expressions for the SOE constants and zone-center vibration frequencies:

$$QC_{11}=-5.112Z'^2+A_1+(A_2+B_2)/2+9.3204Zr_0f_0' \ , \tag{6}$$

$$QC_{12}=0.226Z'^2-B_1+(A_2-5B_2)/4+9.3204Zr_0f_0' \ , \tag{7}$$

$$QC_{44}=2.556Z'^2+B_1+(A_2+3B_2)/4 \ ,$$

$$Q=4r_0^4/e^2 \ , \tag{8}$$

$$\mu w_L^2=R_0'[1+(\tfrac{8}{3}\pi+3\lambda)(\alpha'+\alpha_l')/v] \times[1+(\tfrac{8}{3}\pi+3\lambda)\alpha'/v]^{-1} \ , \tag{9}$$

$$\mu w_T^2=R_0'[1-\tfrac{4}{3}\pi(\alpha'+\alpha_l')/v]\,[(1-\tfrac{4}{3}\pi\alpha'/v)]^{-1} \ ,$$

$$v=2r_0^3 \ , \tag{10}$$

where the abbreviations stand for

$$\alpha'=\sum_{i=1}^{2}\alpha_i'=\sum_{i=1}^{2}\frac{(Y_i'e)^2}{k_i+R_0} \ , \quad d_i'=-\frac{R_0eY_i'}{k_i+R_0} \ , \tag{11}$$

$$\alpha_l'=\frac{(Z'+d_1'-d_2')^2e^2}{R_0'} \ , \tag{12}$$

$$Y_i'=Y_i[Z(Z+12f_0)]^{1/2} \ ,$$

$$R_0=e^2(A_1+2B_1)/v \ , \quad \lambda=16\pi Zr_0f_0'/3Z'^2 \ , \tag{13}$$

$$R_0'=R_0-e^2\left[\frac{d_1'^2}{\alpha_1}+\frac{d_2'^2}{\alpha_2}\right] \ . \tag{14}$$

The symbols (B_1,B_2) and (A_1,A_2) are the usual first and second derivatives of the short-range overlap repulsive energy due to interaction between nn and nnn ions.

A comparison of the Lyddane, Sachs, and Teller's (LST) relation with that obtained from the frequencies given by Eqs. (9) and (10) leads to the following modified Lorentz-Lorenz (LL) and Clausius-Mossotti (CM) relations:

$$\frac{\epsilon-1}{\epsilon+2}=\left[\left(\frac{4\pi}{3}+\lambda\right)\frac{\alpha'}{v}\right]\left[1+\frac{\lambda\alpha'}{v}\right]^{-1} \ , \tag{15}$$

$$\frac{\epsilon_0-1}{\epsilon_0+2}=\left[\left(\frac{4\pi}{3}+\lambda\right)\frac{\alpha'+\alpha_l'}{v}\right]\left[1+\frac{\lambda(\alpha'+\alpha_l')}{v}\right]^{-1} \ , \tag{16}$$

where ϵ and ϵ_0 are the high-frequency and static dielectric constants, respectively. The most striking feature noteworthy from the above relations is that an exactly similar modification in the CM and LL relations has been achieved by Kawaguchi[26] in his microscopic theory of lattice dynamics. These relations clearly demonstrate the effect of TBI on the dielectric properties and the electronic polarizabilities. Substituting $\lambda=0$ reduces the above relations to those obtained within the RSM.

The other important consequence of Eq. (15) is

that it can be directly used to obtain the expression for the strain derivatives of ϵ given in the following form:

$$\left[\frac{r}{\epsilon}\frac{d\epsilon}{dr}\right]_{r=r_0} = -\frac{(\epsilon-1)(\epsilon+2)}{\epsilon(1+\lambda\alpha'/v)} \times\left[1-\frac{r}{3\alpha'}\left(\frac{d\alpha'}{dr}\right)-\frac{r\alpha'}{v} \times\left(\frac{d\lambda}{dr}\right)(\epsilon-1)^{-1}\right]_{r=r_0}, \quad (17)$$

with

$$\left(\frac{d\lambda}{dr}\right)_{r=r_0} = \frac{16\pi}{3ZZ'^2}\left[f_0'-12r_0\left(\frac{f_0'}{Z'}\right)^2+r_0f_0''\right] .$$

Here, $d\alpha'/dr$ is the strain derivative of α', already evaluated by Jaishanker *et al.*[27] for many ionic solids. The second derivative of the three-body force parameter (f_0'') appearing in Eq. (17) is involved in the third space derivative of the crystal energy given by Eq. (1). It is interesting to note that the substitution of only λ and both λ and $d\alpha'/dr$ in the above equation yields expressions equivalent to those derived by Yamashita and Kurosawa[28] and Burstein and Smith,[29] respectively.

Recently, Verma and co-workers[30] have derived the expressions for the third- and fourth-order elastic constants using the homogeneous-deformation method (Wallace[31]). The use of their third-order elastic (TOE) constants and the SOE constants given by Eqs. (6)–(8) leads to the following pressure derivatives of the effective SOE constants (defined by Birch[32]):

$$\frac{dC_{44}'}{dP} = \Omega^{-1}[11.389Z'^2 - A_1 + 3B_1 - \tfrac{1}{4}(C_2+2A_2-10B_2) - 44.652Zr_0f_0'] , \quad (18)$$

$$\frac{dS'}{dP} = \Omega^{-1}[-11.838Z'^2 - \tfrac{1}{2}C_1 - \tfrac{1}{8}(C_2+6A_2-6B_2) + 25.537Zr_0f_0' - 6.99Zr_0^2f_0''] , \quad (19)$$

$$\frac{dK'}{dP} = \Omega^{-1}[-4.658Z'^2 + A_1 + A_2 - \tfrac{1}{3}(C_1+C_2) + 55.921Zr_0f_0' - 13.98Zr_0^2f_0''] . \quad (20)$$

Here, the abbreviations stand for

$$S' = \tfrac{1}{2}(C_{11}'-C_{12}') , \quad K' = \tfrac{1}{3}(C_{11}'+2C_{12}') ,$$

$$\Omega = -2.33Z'^2 + A_1 + A_2 + 27.961Zr_0f_0' . \quad (21)$$

Also, C_1 and C_2 are the repulsive parameters due to the interaction between nn and nnn ions, respectively. They are defined as

$$C_1 = Q\left[\frac{rd^3\Phi_1^R(r)}{dr^3}\right]_{r=r_0} = A_1^2/B_1 , \quad (22)$$

$$C_2 = Q\left[\frac{rd^3\Phi_2^R(r)}{dr^3}\right]_{r=\sqrt{2}r_0} = A_2^2/B_2 \quad (23)$$

and related to the other short-range parameters as indicated above. This relationship makes them as redundant parameters. The strategy for the determination of model parameters and the results obtained from them are presented in Sec. III.

TABLE I. Input data for sodium halides. SOE constants, lattice parameter, and electronic polarizabilities are for 0 °K temperature, pressure derivatives are given at 295 °K and zone-center vibration frequencies for NaF and NaBr are at room temperature and those for NaCl and NaI are, respectively, at 80 and 100 °K.

Constants	NaF values	Ref.	NaCl values	Ref.	NaBr values	Ref.	NaI values	Ref.
C_{11} (10^{11} dyn cm^{-2})	11.894	a	5.733	65	4.800	65	3.761	65
C_{12} (10^{11} dyn cm^{-2})	2.290	65	1.123	65	0.986	65	0.798	65
C_{44} (10^{11} dyn cm^{-2})	2.899	65	1.331	65	1.070	65	0.781	65
r_0 (Å)	2.3040	65	2.7978	65	2.9601	65	3.2044	65
α_1 (Å^3)	0.290	65	0.290	65	0.290	65	0.290	65
α_2 (Å^3)	0.858	65	2.946	65	4.090	65	6.114	65
$\frac{dK'}{dP}$	5.180	64	5.270	64	5.290	64	5.400	64
ν_L (10^{12} sec^{-1})	12.650	33	7.830	34	6.220	35	5.170	36
ν_T (10^{12} sec^{-1})	7.510	33	5.172	34	4.040	35	3.600	36

[a]Calculated from compressibility value (Ref. 47) ($\beta = 1.821\times10^{-12}$ cm^2/dyne at 0 °K) using the relation $\beta = 3(C_{11}+2C_{12})^{-1}$.

TABLE II. Model parameters for sodium halides.

Parameters	NaF	NaCl	NaBr	NaI
A_1	10.541 63	11.000 26	11.065 54	11.459 11
B_1	−1.029 46	−1.081 23	−1.057 92	−1.069 24
A_2	0.533 49	0.351 57	0.464 16	0.437 95
B_2	−0.036 84	−0.024 43	−0.031 38	−0.028 90
d_1'	0.031 90	0.005 52	0.037 68	0.033 71
d_2'	0.134 39	0.232 19	0.278 42	0.351 28
Y_1'	−3.152 19	−10.605 76	−1.328 02	−1.218 32
Y_2'	−2.214 02	−2.559 97	−2.534 40	−2.465 16
f_0	−0.007 06	−0.004 24	−0.005 42	−0.004 78
$r_0 f_0'$	−0.031 93	−0.023 71	−0.011 99	0.003 33
$r_0^2 f_0''$	0.134 86	−0.005 77	−0.022 89	−0.146 39

III. COMPUTATIONS AND RESULTS

The model described in Sec. II contains 11 parameters (A_1, B_1, A_2, B_2, d_1', d_2', Y_1', Y_2', f_0, $r_0 f_p'$, and $r_0^2 f_0''$). The essential starting step for their determination is the method of successive approximation to choose a suitable value of ρ on the basis of arguments provided earlier by Puri and Verma.[30] The use of the equilibrium condition

$$B_1 + B_2 = -1.165 Z'^2 \ , \tag{24}$$

together with Eqs. (6)–(14) and (20) enables one to obtain all 11 parameters. The input data used for their calculation are listed in Table I together with their relevant references and temperatures. The values of the model parameters are given in Table II and used to obtain the phonon spectra by solving the secular equation (2) corresponding to 48 nonequivalent points in the first Brillouin zone. The physical properties derived from these spectra have been described below.

1. *Lattice-dynamic properties*

The phonon spectra obtained above have been used to predict the phonon dispersion relations $w_j(q)$ which are measured from inelastic neutron scattering and provide the most dependable test of any model.

(i) Phonon dispersion relations. The phonon dispersion relations along principal symmetry directions have been displayed in Figs. 1–4 and compared with their neutron data.[33–36] The results obtained from the deformation shell model[37] have also been displayed in these for visual comparison. The agreement shown

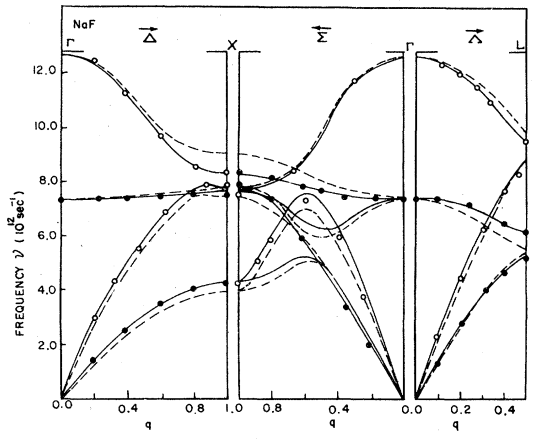

FIG. 1. Phonon dispersion curves of NaF. Theoretical curves: solid line, TSM; dashed line, DSM (Ref. 37). Experimental points at room temperature (Ref. 33): ○, longitudinal; ●, transverse.

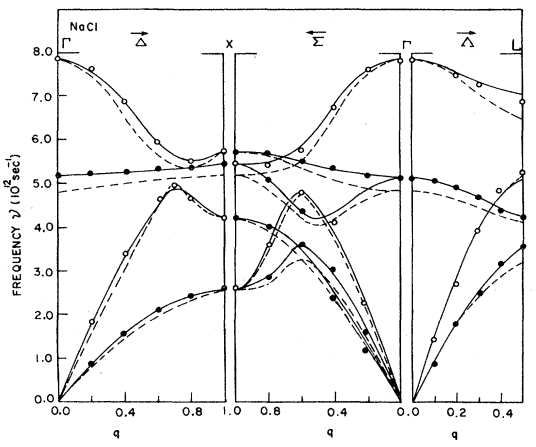

FIG. 2. Phonon dispersion curves of NaCl. Theoretical curves: solid line, TSM, dashed line, DSM (Ref. 37). Experimental points at 80 °K (Ref. 34): ○, longitudinal; ●, transverse.

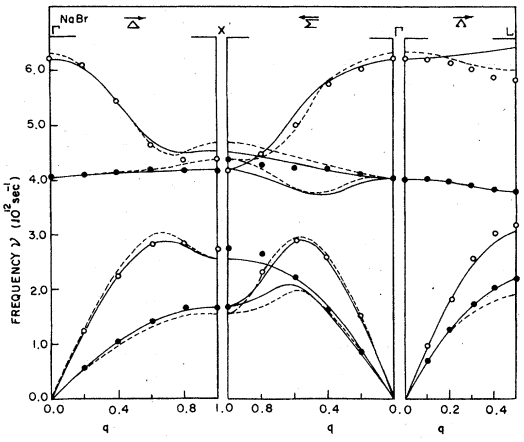

FIG. 3. Phonon dispersion curves of NaBr. Theoretical curves: solid line, TSM; dashed line, DSM (Ref. 37). Experimental points at room temperature (Ref. 35): ○, longitudinal; ●, transverse.

by the TSM is distinctly better than that obtained by the deformation shell model except for the LO branch along the [111] direction, particularly for NaBr and NaI. This feature of the TSM is not surprising because the elements of the three-body dynamical matrix reported by Verma and Singh[7] tend to increase the vibration frequencies along the [111] direction in going from the Γ to the L point, especially in the case of solids whose ions differ strongly in size. A similar feature has been exhibited by the microscopic TSM developed by Zeyher.[13] The cause for such large deviations has been ascribed to the presence of some additional polarization mechanism which lowers the longitudinal-optical frequencies along the (111) direction in such solids. He has thus concluded that an additive inclusion of three-body terms in the RSM cannot bring improvement over it, particularly for this branch. However, these deviations can be reduced drastically by more extensive inclusion of nnn interactions, as pointed out by Singh and Verma[38] and done by Singh and Chandra.[25] The minor deviations are expected to disappear if the predicted phonon frequencies are measured by neutron spectroscopy at lower temperatures for which the equilibrium condition of the model holds.

The dispersion curves of NaF (Ref. 33) have been analyzed with other pre[3]- and post[13,18,38–40]-experimental models. The agreements achieved are moderately good in most cases. The dispersion of phonons in NaCl has been studied by various other theoretical models[3,13,38–45] developed before and after the experimental measurements.[34,46,47] The successful ones among them are, generally, the polarizable models[2,3] and their variants.[4–6,13] Some of these models have also been applied by various workers[35,38,45] to predict the phonon dispersion in NaBr.[35] Attempts[2–5,38] have also been made to explain the dispersion relations in NaI,[36] but most of the models failed to reproduce the longitudinal-optical branch along the [111] direction.

(ii) Two-phonon Raman and ir spectra. The computed phonon spectra have been used to explain the two-phonon Raman and ir spectra following the combined density of states (CDS) approach (Smart

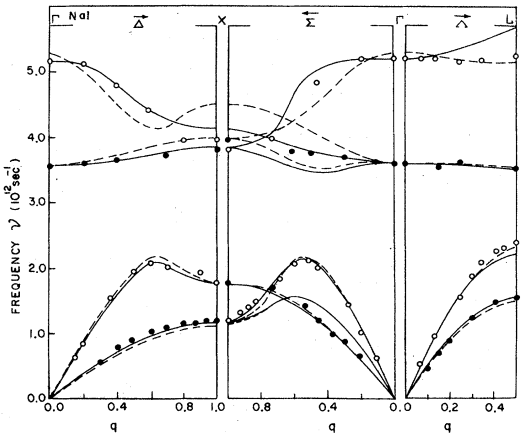

FIG. 4. Phonon dispersion curves of NaI. Theoretical curves: solid line, TSM; dashed line, DSM (Ref. 37). Experimental points at 100°K (Ref. 36): ○, longitudinal; ●, transverse.

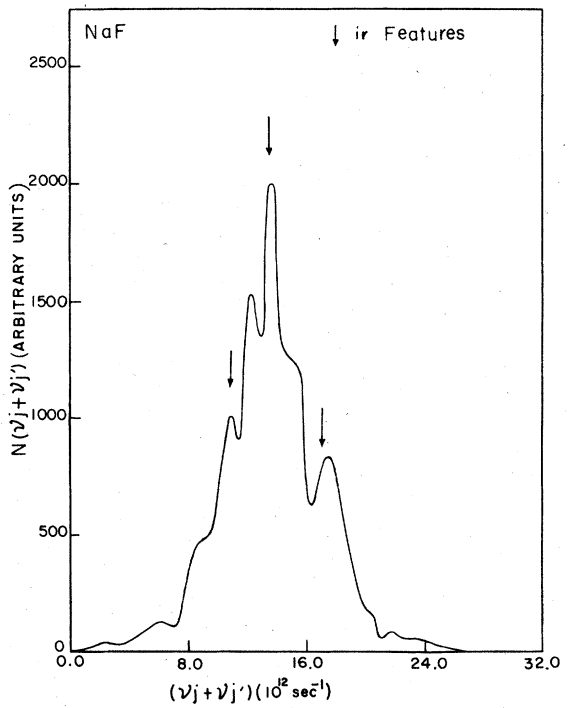

FIG. 5. Combined density of states curve for NaF. Observed ir peaks at 100°K (Ref. 48) are shown by solid arrows.

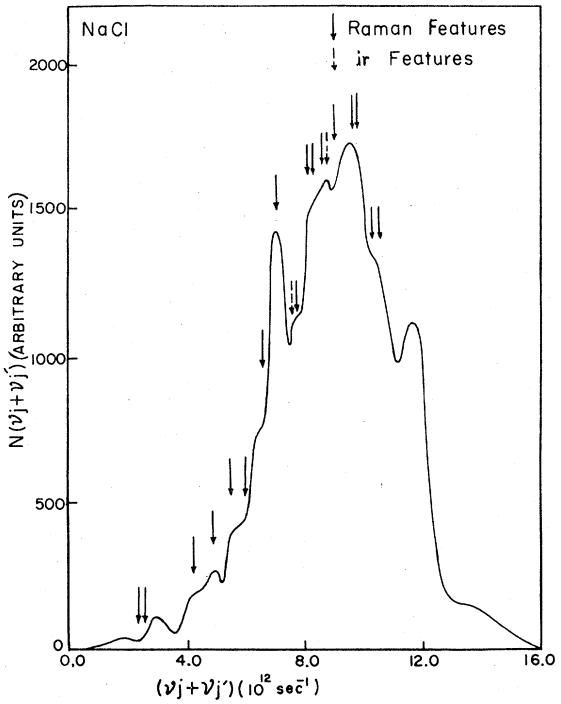

FIG. 6. Combined density of curve for NaCl. Observed Raman shifts at 300°K: solid arrows (Ref. 50); observed ir peaks at 300°K; broken arrows (Ref. 48).

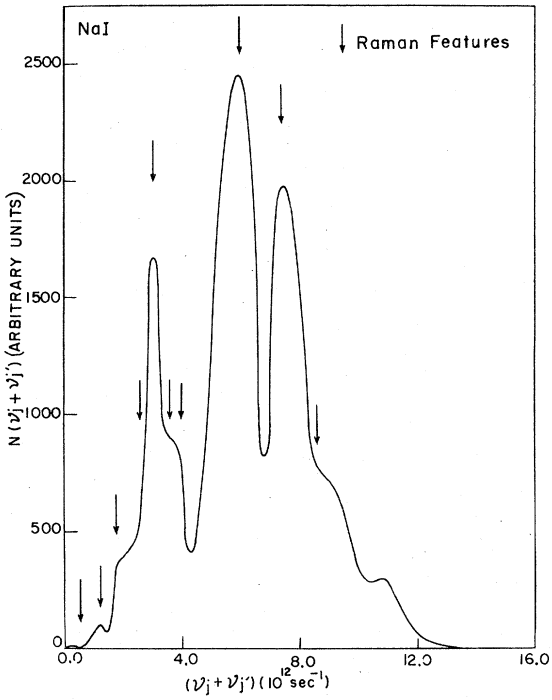

FIG. 8. Combined density of states curve for NaI. Observed Raman shifts at 300°K (Ref. 51) are shown by solid arrows.

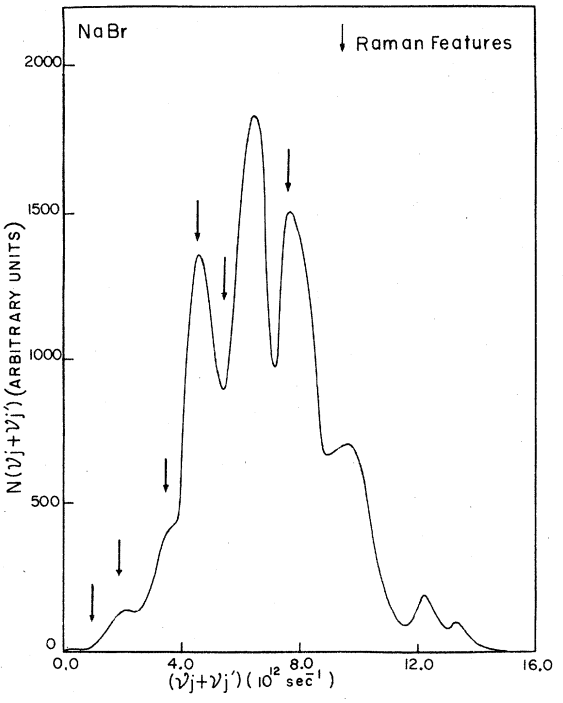

FIG. 7. Combined density of states curve for NaBr. Observed Raman shifts at 300°K (Ref. 50) are shown by solid arrows.

et al.[48]) and critical-point analysis (Burstein *et al.*[49]). The CDS curves have been displayed in Figs. 5–8. The agreements achieved between theoretical and experimental[48,50,51] peaks is generally good.

In order to interpret the fine structure of Raman spectra, we have carried out the critical-point analysis. The assignments achieved have been listed in Tables III and IV together with their observed data. The peaks assigned by the present model are found to agree fairly well with those observed in Raman and ir experiments. This detailed investigation is intended to provide a reliable test particularly for the higher range of frequency spectra revealed by the TSM. These studies will also be useful in connecting the neutron and optical data and explaining the coupling between the modes of vibrations of the ions (Barnes *et al.*[52]).

(iii) Debye-temperature variations. The Debye-temperatures have been derived in the usual way from the specific heats which are sensitive to the lower range of phonon spectra. They have been plotted as functions of the temperatures in Fig. 9 and compared with their experimental results available only for NaCl[53] and NaI.[54] The agreement between theoretical and experimental results is almost excellent throughout except at higher temperatures. The inclusion of anharmonic effects in the model might improve this reproduction.

TABLE III. Assignments of two-phonon Raman and ir spectra for NaF and NaCl in units of cm^{-1}

Observed peaks (Ref. 48)[a]	NaF (ir) values	Theoretical peaks assignments		NaCl (Raman) values	Observed peaks (Ref. 50)[b]
370	378	$TO(L)+TA(L)$	$LO(L)-TO(L)$	93	85
452	466	$LA(L)+TA(L)$	$LO(L)-TA(L)$	120	135,140
566	555	$2LO(X)$	$2TA(X)$	167	162
			...	...	184,202
	NaCl (ir)[b]		$La(X)+TA(X)$	224	220
80	88	$LO(\Gamma)-TO(\Gamma)$	$2TA(L)$	234	235
236	234	$2TA(L)$	$TO(L)+TA(L)$	260	258
254	260	$TO(L)+TA(L)$	$LO(X)+TA(X)$	277	270,276
292	287	$2TO(L)$	$LA(L)+TA(L)$	286	286
			...	...	300
			$TO(L)+LA(L)$	313	314,320
			$TO(X)+LA(X)$	323	326
			$2TO(\Gamma)$	345	343
			$LO(L)+TA(L)$	353	350

[a]Experimental measurements are at 100 °K.
[b]Experimental measurements are at 300 °K.

(iv) Dielectric and photoelastic properties. In this paper the dielectric constants have been calculated from the model parameters and listed in Table V. The values calculated from the TSM are in excellent agreement with their measured data[55] as is evident from the table. The results obtained for the strain derivatives of ϵ have also been listed in the same table. They have been compared with other theoretical[27,29,56,57] and experimental data.[57] The experimental results are available only for NaCl.[57] The agreement achieved by us is adequately satisfactory as it is much better than those revealed by several other

TABLE IV. Assignments of two-phonon Raman spectra for NaBr and NaI in units of cm^{-1}.

Observed peaks[a] (Ref. 50)	NaBr values	Theoretical peaks assignments		NaI values	Observed peaks[a] (Ref. 51)
31	30	$LA(L)-TA(L)$	$LA(X)-TA(X)$	19	19
64	67	$LO(X)-LA(X)$	$TO(L)-LA(L)$	44	42
116	114	$LO(L)-LA(L)$	$TO(L)-TA(L)$	65	58
152	149	$2TA(L)$	$TO(X)-TA(X)$	89	88
181	177	$LA(L)+TA(L)$	$2TA(L)$	104	103
254	254	$2TO(L)$	$2LA(X)$	117	120
			$LO(L)-TA(L)$	136	132
			$LO(X)+LA(X)$	196	200
			$2TO(L)$	234	200–250
			$2TO(\Gamma)$	240	...
			$LO(L)+TA(L)$	241	...
			$2TO(X)$	255	...
			$2LO(\Gamma)$	345	310–370
			$2LO(L)$	378	...

[a]Experimental measurements are at 300 °K.

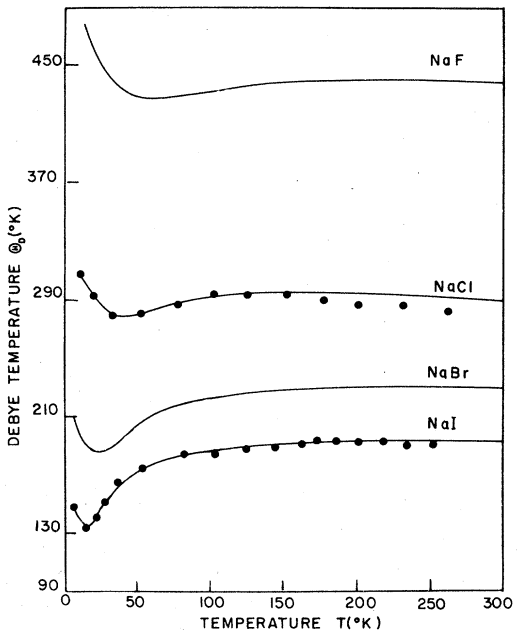

FIG. 9. Debye-temperature variations as functions of temperature for sodium halides. Theoretical curves, TSM. Experimental points; NaCL (•, Ref. 53); NaI (•, Ref. 54).

models listed in Table V.

(v) Elastic properties. The TOE constants have been calculated and listed in Table VI together with theoretical[59–62] and experimental[58–63] results. The present TSM results have shown fairly good agreement with measured data. It is interesting to note that our results are generally better than those of others as is evident from the table. However, the results of Garg *et al.*[61] are closer to the experimental values,[53,58] but their parameters are limited by explaining only the elastic properties. It can also be seen from Tables I and VI that the Cauchy discrepancy expressed in percent is smaller for the TOE constants than for the SOE constants. A possible explanation for this fact seems to be that many-body and/or, thermal effects are more pronounced for SOE than for TOE constants.

The pressure derivatives of the effective SOE constants calculated by us have been given in Table VI and found to be generally in good agreement with their observed data.[66] However, the agreement with the TSM is poor for dC_{44}'/dP. The agreement might improve if the lower-temperature data are used for comparison. Unfortunately, values at lower temperatures are not available.

2. *Lattice static properties*

The model parameters employed in the above descriptions have been used to study the static properties of sodium-halide crystals. This has been done by expressing the cohesive energy per unit cell for the TSM as

$$\Phi_{\mathrm{NaCl}}=\frac{\alpha_{\mathrm{NaCl}}Z^2e^2}{r}+6\frac{\alpha_{\mathrm{NaCl}}Z^2e^2}{r}f(r)+6be^{-r/\rho} \tag{25}$$

and the same expression for the hypothetical (CsCl structure) lattice as

$$\Phi_{\mathrm{CsCl}}=\frac{\alpha_{\mathrm{CsCl}}Z^2e^2}{r}+8\frac{\alpha_{\mathrm{CsCl}}Z^2e^2}{4}f(r)+8be^{-r/\rho}\ . \tag{26}$$

The cohesive energy can be calculated for the NaCl phase from Eq. (25) with the knowledge of the parameters b, ρ, and $f(r)$. Now, considering these parameters to be structure independent and imposing

TABLE V. Static and high-frequency dielectric constants (ϵ_0, ϵ) and strain derivative of ϵ. The experimental values correspond to 2 °K measurements.

Crystal	ϵ_0		ϵ		$\left[\left(\frac{r}{\epsilon}\right)\left(\frac{d\epsilon}{dr}\right)\right]_{r=r_0}$		
	Present	Expt. (55)	Present	Expt. (55)	Theoretical	Present	Expt. (57)
NaF	4.639	4.73	1.642	1.75	−0.64,[a] −1.59,[b] −1.27,[c] −1.16[d]	−0.410	···
NaCl	5.079	5.45	2.215	2.35	−0.80,[a] −2.47,[b] −1.85,[c] −1.53[d]	−0.869	−0.95[d]
NaBr	6.060	5.78	2.561	2.64	−1.31,[a] −2.83,[b] −2.04,[c] −1.64[d]	−1.334	···
NaI	6.384	6.62	3.093	3.08	−1.76,[a] −3.35,[b] −2.33,[c] −1.76[d]	−2.168	···

[a]Reference 27. [b]Reference 29. [c]Reference 56. [d]Reference 57.

TABLE VI. TOE constants (10^{12} dyn cm^{-2}) and pressure derivatives of SOE constants (dimensionless). Experimental values are at 295 °K.

Crystal	Source	C_{111}	C_{112}	C_{123}	C_{144}	C_{166}	C_{456}	$\frac{dC'_{44}}{dP}$	$\frac{dS'}{dP}$
NaF	Expt. (58)	−14.80	−2.70	2.80	0.46	−1.14	0.00	0.205[a]	4.79[a]
	Present	−21.01	−0.90	0.40	0.47	−1.16	0.51	−0.025	5.18
	Theo. (59)	−7.14	−1.44	0.56	0.76	−1.28	0.76	0.110	1.58
	Theo. (60)	−8.56	−1.39	0.56	0.56	−1.43	0.54	0.470	···
	Theo. (61)	−16.45	−1.36	0.39	0.44	−1.16	0.47	0.147	···
	Theo. (62)	−19.83	−0.65	0.23	0.56	−1.36	0.59	···	···
NaCl	Expt. (63)	−8.80	−0.57	0.28	0.26	−0.61	0.27	0.370[a]	4.79[a]
	Present	−10.23	−0.47	0.21	0.23	−0.52	0.25	−0.159	5.25
	Theo. (59)	−5.45	−0.69	0.27	0.36	−0.63	0.35	0.220	2.78
	Theo. (60)	−8.61	−0.52	0.16	0.26	−0.57	0.25	0.080	···
	Theo. (61)	−8.38	−0.67	0.17	0.17	−0.61	0.17	0.306	···
	Theo. (62)	−8.70	−0.68	0.09	0.27	−0.85	0.27	···	···
NaBr	Expt. (64)	···	···	···	···	···	···	0.46	4.83
	Present	−8.64	−0.41	0.17	0.19	−0.42	0.19	−0.182	5.22
	Theo. (60)	−6.62	−0.41	0.13	0.20	−0.45	0.19	−0.013	···
	Theo. (61)	−6.92	−0.58	0.14	0.13	−0.53	0.12	0.436	···
NaI	Expt. (64)	···	···	···	···	···	···	0.610	4.80
	Present	−6.89	−0.34	0.14	0.14	−0.31	0.14	−0.276	5.29
	Theo. (60)	−4.51	−0.30	0.09	0.15	−0.34	0.14	0.060	···
	Theo. (61)	−5.28	−0.47	0.09	0.08	−0.48	0.07	0.798	···

[a]Reference 64.

on Eq. (26) the equilibrium condition

$$\left(\frac{d\Phi_{CsCl}}{dr}\right)_{r=r_0}=0 \ , \tag{27}$$

we get the new value of r_0 whose substitution in Eq. (28) gives the cohesive energy for the hypothetical lattice. The values of the cohesive energies listed in Table VII have predicted all the structures correctly. This shows that the TSM is capable of explaining the relative stability of the system of solids under consideration. Also, the cohesive energy obtained from the TSM is much closer to the experimental values[69] than those obtained by others.[66–68]

Since the atomization energy (E_a) gives a better idea of the stability of a crystal than the cohesive energy we have therefore calculated it by using the expression $E_a=\Phi+E-I$ with E and I as the electron affinity of the anion and the ionization energy of the cation, respectively. The atomization energy has been calculated and listed in Table VII (using E and I as reported by Kothari and Rao[75]), together with other experimental[70] and other theoretical[71] values. The TSM results are generally better than those given by others.[71]

The phase-transition pressure between the two phases 1 and 2 for any solid at a temperature T is obtained from the condition that the Gibbs free energy is the same at the transition pressure. Thus, following Gibbs notation, we can write

$$U_1+pv_1-TS_1=U_2+pv_2-TS_2 \ . \tag{28}$$

At low temperature, we may consider $T\approx 0$ and the internal energy U to be cohesive energy Φ_0. The phase-transition pressure from Eq. (28) is given by

$$p=(\Phi_2-\Phi_1)/(v_1-v_2) \ , \tag{29}$$

with v_1-v_2 as the corresponding phase-transition volume per unit cell, and can be obtained from the values of r_0 in phases 1 and 2. The phase-transition pressure and volume have been calculated by using Eq. (29) from the knowledge of Φ_1 and Φ_2 given in Table VII. The results have been listed in Table VII

TABLE VII. Cohesive and atomization energy and phase-transition pressure and volume.

Crystal	Structure	Cohesive energy (kcal/mole) Theoretical Ref. 68	Cohesive energy (kcal/mole) Theoretical Present	Cohesive energy (kcal/mole) Experimental Ref. 69[b]	Atomization energy (kcal/mole) Theoretical Ref. 70[c]	Atomization energy (kcal/mole) Theoretical Present	Atomization energy (kcal/mole) Theoretical Ref. 71	Phase-transition pressure (kbar) Theoretical Ref. 68	Phase-transition pressure (kbar) Theoretical Present	Phase-transition pressure (kbar) Expt.[a]	Phase-transition volume (cm^3/mole) Present
NaF	NaCl	211.9	219.3	217.9	193.7	181.3	176.3	326,15.6[g]	106.8	>200[d]	3.495
	CaCl	203.1	210.4								
NaCl	NaCl	179.9	183.1	185.3	153.1	148.8	152.7	107	44.6	300[e]	5.629
	CsCl	173.9	177.1								
NaBr	NaCl	173.8	172.6	174.3	139.5	132.6	127.9	79	39.2	>100[f]	6.055
	CsCl	168.8	166.9								
NaI	NaCl	164.9	160.4	162.3	120.8	113.5	119.4	23	32.0	>100[f]	6.317
	CsCl	162.5	155.5								

[a]Experimental measurements are at 0 °K.
[b]Extrapolated to 0 °K by L. Brewer, quoted by Kittle, (see Ref. 69).
[c]These values are at room temperatures.
[d]Reference 72.
[e]Reference 73.
[f]Reference 74.
[g]Reference 19.

and compared with the experimental[72–74] and other theoretical[18,68] values. The agreements achieved with the TSM are not better than those of Cohen and Gordon[68] but they are definitely better than those reported by Ghosh *et al.*[19] However, the calculated and measured values differ appreciably in their magnitudes in all the cases. This situation might improve by incorporating the corrections due to the temperature which is responsible for the phase transition.

IV. SUMMARY AND CONCLUSIONS

The primary purpose of this paper is to carry out a consistent and comprehensive calculation of the lattice statics and dynamics of ionic crystals. The aim has been achieved by applying the TSM to study the phonon-dispersion, harmonic elastic, dielectric, photoelastic anharmonic elastic and static (cohesion, relative stability, and phase transition) properties of sodium halides. A reasonably good agreement revealed by the TSM for all these properties may be considered, remarkable in view of the fact that the same set of model parameters has been used throughout the calculations.

On the basis of an overall analysis, the TSM may be regarded as an adequate and appropriate model to describe the lattice statics and dynamics of ionic crystals. The discrepancies between theory and experiment may be eliminated by including (a) the effect of the short-range three-body potential, (b) the zero-point motion of cores, and (c) the Van der Waals interactions, and the anharmonic corrections. The success of the TSM predictions of a large body of crystal properties may be considered adequate to give us confidence in the TSM even though it involves many parameters.

ACKNOWLEDGMENTS

The authors are grateful to the University Grants Commission (UGC), Delhi, for the financial support of this project. One of us (V.V.S.N.) is thankful to Principal D. P. S. Verma for encouragements and to U. G. C. for a Teacher Fellowship.

[1]E. W. Kellermann, Phil. Trans. R. Soc. London Ser. A 238, 513 (1940).
[2]A. D. B. Woods, W. Cochran, and B. N. Brockhouse, Phys. Rev. 119, 980 (1960).
[3]A. M. Karo and J. R. Hardy, Phys. Rev. 129, 2024 (1963).
[4]U. Schröder, Solid State Commun. 4, 347 (1966).
[5]A. N. Basu and S. Sengupta, Phys. Status Solidi 29, 367 (1968).

[6]R. Srinivasan, G. Laxmi, and V. Ramchandran, J. Phys. C 8, 2889 (1975); 8, 2897 (1975); L. A. Feldkamp. J. Phys. Chem. Solids 33, 711 (1972).
[7]M. P. Verma and R. K. Singh, Phys. Status Solidi 33, 769 (1969).
[8]K. B. Tolpygo, Sov. Phys. Solid State 3, 685 (1961).
[9]V. V. Mitakevitch, Fiz. Tverd. Tela (Leningrad) 3, 3022 (1961) [Sov. Phys. Solid State 3, 2202 (1962)].
[10]R. A. Cowley, Proc. R. Soc. London Ser. A 268, 121 (1962).
[11]S. K. Sinha, Phys. Rev. 169, 477 (1968); 177, 1256 (1969).
[12]F. A. Johnson, Proc. R. Soc. London Ser. A 310, 79 (1969); A 310, 89 (1969); A 310, 101 (1969).
[13]R. Zeyher, Phys. Status Solidi B 48, 711 (1971).
[14]R. M. Pick, M. H. Cohen, and R. M. Martin, Phys. Rev. B 1, 910 (1970).
[15]P. O. Löwdin, Ark. Mat. Astron. Fys. A 35, 30 (1947).
[16]S. O. Lundqvist, Ark. Fys. 6, 25 (1952); 9, 435 (1955); 12, 263 (1957); 19, 113 (1961).
[17]A. Herpin, J. Phys. Radium 14, 611 (1953).
[18]A. N. Basu, D. Roy, and S. Sengupta, Phys. Status Solidi A 23, 11 (1974).
[19]A. Ghosh, A. N. Basu, and S. Sengupta, Proc. R. Soc. London Ser. A 340, 199 (1974).
[20]A. Ghosh and A. N. Basu, Phys. Status Solidi 36, 359 (1968); Phys. Rev. B 14, 4616 (1976).
[21]A. K. Sarkar and S. Sengupta, Solid State Commun. 7, 135 (1969); Phys. Status Solidi 36, 359 (1969); B 58, 775 (1973).
[22]D. Laplaze, J. Phys. C 10, 3499 (1977).
[23]S. C. Goyal, L. D. Agrawal, and M. P. Verma, Phys. Rev. B 10, 779 (1974).
[24]S. C. Goyal, R. Prakash, and S. P. Tripathi, Phys. Status Solidi B 85, 477 (1978).
[25]R. K. Singh and K. Chandra, Phys. Rev. B 14, 2625 (1976).
[26]H. Kawaguchi (private communication).
[27]Jai Shanker, S. C. Agrawal, and O. P. Sharma, J. Chem. Phys. 67, 5452 (1977).
[28]J. Yamashita and T. Kurosawa, J. Phys. Soc. Jpn. 10, 610 (1955).
[29]E. Burstein and P. L. Smith, Phys. Rev. 74, 229 (1948).
[30]D. S. Puri and M. P. Verma, Phys. Status Solidi B 78, 113 (1976); 63, 80(i) (1977); Phys. Rev. B 15, 2337 (1977).
[31]D. C. Wallace, *Thermodynamics of Crystals* (Wiley, New York, 1972).
[32]F. Birch, Phys. Rev. 71, 809 (1947).
[33]W. J. L. Buyers, Phys. Rev. 153, 923 (1967).
[34]G. Raunio, L. Almqvist, and R. Stedman, Phys. Rev. 178, 1496 (1969).
[35]J. S. Reid, T. Smith, and W. J. L. Buyers, Phys. Rev. B 1, 1833 (1970).
[36]R. A. Cowley, W. Cochran, B. N. Brockhouse, and A. D. B. Woods, Phys. Rev. 131, 1630 (1963).
[37]J. S. Melvin, J.D. Pierie, and T. Smith, Phys. Rev. 175, 1082 (1968).
[38]R. K. Singh and M. P. Verma, Phys. Rev. B 2, 4288 (1970).
[39]V. V. Namjoshi, S. S. Mitra, and J. F. Vetelino, Solid State Commun. 9, 185 (1971).
[40]Sneh and B. Dayal, Phys. Status Solidi B 67, 125 (1975).
[41]R. F. Schmunk, Bull. Am. Phys. Soc. 12, 281 (1967).
[42]V. Nusslin and U. Schröder, Phys. Status Solidi 21, 309 (1967).
[43]Lagu and Dayal, Ind. J. Pure Appl. Phys. 6, 670 (1968).
[44]G. Raunio and S. Rolandson, Phys. Rev. B 2, 2098 (1970).
[45]A. N. Basu and S. Sengupta, Phys. Rev. B 8, 2982 (1973).
[46]A. M. Karo and J. R. Hardy, Phys. Rev. 181, 1272 (1969).
[47]A. M. Karo and J. R. Hardy, Phys. Rev. 141, 696 (1966); 160, 702 (1967).
[48]C. Smart, G. R. Wilkinson, A. M. Karo, and J. R. Hardy, in *Lattice Dynamics,* edited by R. F. Wallis (Pergamon, Oxford, 1965).
[49]E. Burstein, F. A. Johnson, and R. London, Phys. Rev. 139, 1239 (1965).
[50]R. S. Krishnan, in *Lattice Dynamics,* edited by R. F. Wallis (Pergamon, Oxford, 1965).
[51]R. S. Krishnan and N. Krishnamurthy, Z. Phys. 175, 440 (1963).
[52]R. H. Barnes, R. Brattain, and F. Szigeti, Phys. Rev. 48, 582 (1935).
[53]K. Clusius, J. Goldmann, and A. Perlick. Z. Naturforsch Teil A 4, 424 (1949).
[54]W. T. Berg and J. A. Morrison, Proc. R. Soc. London Ser. A 242, 467 (1957).
[55]R. P. Löwndes and D. H. Martin, Proc. R. Soc. London Ser. A 308, 473 (1969).
[56]R. Srinivasan and K. Srinivasan, J. Phys. Chem. Solids 33, 1079 (1972); Phys. Status Solidi B 57, 757 (1973).
[57]J. A. Van Vechten, Phys. Rev. 182, 891 (1969).
[58]W. A. Bensch, Phys. Rev. B 6, 1504 (1972).
[59]A. A. Nran'yan, Sov. Phys. Solid State 5, 129 (1963).
[60]P. B. Ghate, Phys. Rev. A 139, 1666 (1965).
[61]V. K. Garg, D. S. Puri, and M. P. Verma, Phys. Status Solidi B 80, 63 (1977).
[62]S. Paul, Ind. J. Pure Appl. Phys. 8, 307 (1970).
[63]Z. P. Chang, Phys. Rev. 140, A1788 (1965).
[64]R. W. Roberts and C. S. Smith, J. Phys. Chem. Solids 31, 619 (1970).
[65]J. R. Hardy and A. M. Karo, Solid State Phys. (to be published).
[66]R. K. Singh and V. V. S. Nirwal, Nuovo Cimento 22, 559 (1978).
[67]O. P. Sharma, A. P. Gupta, and Jaishanker, Phys. Status Solidi B 83, K13 (1977).
[68]A. J. Cohen and R. G. Gordon, Phys. Rev. B 12, 3228 (1975).
[69]C. Kittle, *Introduction to Solid State Physics,* 4th ed. (Wiley, New York, 1971), p. 121.
[70]F. Seitz, *Modern theory of solids* (McGraw-Hill, New York, 1940), p. 47.
[71]K. P. Thakur, Aust. J. Phys. 29, 46 (1976).
[72]Y. S. Kim and R. G. Gorden, Phys. Rev. B 9, 3548 (1974).
[73]W. A. Bassett, T. Takahashi, H. K. Mao, and J. S. Weaver, J. Appl. Phys. 39, 319 (1968).
[74]M. Born and K. Huang, *Dynamic Theory of Crystal Lattices* (Oxford University, London, 1954), p. 162.
[75]L. S. Kothari and C. N. R. Rao, *Basic Physical and Chemical data* (East West, India, 1970), p. 33,35.